Light-controlled photonics-based mm-wave beam switch

VLADIMIR YURCHENKO,[1,*] MEHMET CIYDEM,[1] MARCIN GRADZIEL,[2] ANTHONY MURPHY,[2] AND AYHAN ALTINTAS[2]

[1]*Engitek Engineering Technologies Ltd, 197/16 Ceyhun Atif Kansu, 06460, Ankara, Turkey*
[2]*Experimental Physics Department, Maynooth University, Maynooth, Ireland*
[3]*EEE Department, Bilkent University, 06800, Ankara, Turkey*
[*]*v.yurchenko@nuim.ie*

Abstract: We present experimental investigation of light-controlled photonics-enhanced quasi-optical mm-wave beam switch operating at a resonant frequency in the mm-wave band of 75 to 110 GHz. The switch is implemented as a Bragg structure with a resonant layer of high-resistivity silicon that creates a narrow transmission peak within the mm-wave propagation gap. The peak amplitude is sensitive to the intensity of light pulses illuminating the structure. When using a silicon wafer of 30 KOhm · cm resistivity and light pulses created by a 400 W LED-array light source, we achieved mm-wave transmission peak modulation exceeding 15 dB.

References and links

1. A. A. Vikharev, G. C. Denisov, V. V. Kocharovskii, S. V. Kuzikov, V. V. Parshin, N. Y. Peskov, A. N. Stepanov, D. I. Sobolev, and M. Y. Shmelev, "A high-speed quasi-optical wave phase switch based on the induced photoconductivity effect in silicon," Tech. Phys. Lett. **33**(9), 735–737 (2007).
2. L. Fekete, F. Kadlec, P. Kuzel, and H. Nemec, "Ultrafast opto-terahertz photonic crystal modulator," Opt. Lett. **32**(6), 680–682 (2007).
3. I. Chatzakis, P. Tassin, L. Luo, N. H. Shen, L. Zhang, J. Wang, T. Koschny, and C. M. Soukoulis, "One- and two-dimensional photo-imprinted diffraction gratings for manipulating terahertz waves," Appl. Phys. Lett. **103**, 043101 (2013).
4. S. M. Sze, *Semiconductor Devices, Physics and Technology* (John Wiley and Sons, 2002)
5. V. B. Yurchenko, M. Ciydem, M. Gradziel, J. A. Murphy, and A. Altintas, "Double-sided split-step mm-wave Fresnel lenses: fabrication and focal field measurements," J. European Opt. Soc.-Rapid Publ. **9**, 14007 (2014).
6. V. B. Yurchenko, M. Ciydem, and A. Altintas, "Light-controlled microwave whispering-gallery-mode quasi-optical resonators at 50W LED array illumination," AIP Advances **5**, 087144 (2015).
7. H. Guo, J. Chen, and S. Zhuang, "Vector plane wave spectrum of an arbitrary polarized electromagnetic wave," Optics Express **14**(6), 2095–2100 (2006).
8. G. Zhou, X. Chu, and J. Zheng, "Analytical structure of an apertured vector Gaussian beam in the far field," Optics Commun. **281**, 1929–Âŋ1934 (2008).

1. Introduction

Optical control of THz and sub-THz beams is a promising way of ultra-fast switching, modulation, and other processing of electromagnetic waves of millimeter (mm) and sub-millimeter (sub-mm) wave bands [1–3]. In this way, a nanosecond-fast light-controlled phase inversion in a 30 GHz quasi-optical beam is achieved [1] using the photoconductivity effect in a silicon wafer placed on top of metallic mirror. A high-power Ti:sapphire laser has been used in that study, with laser beam re-focused over the entire silicon surface.

Light sensitivity could be enhanced with quasi-optical resonators using photoconductive elements that control the wave propagation. In [2], Fekete et al present a THz device with enhanced sensitivity due to the use of Bragg structure with GaAs inner layer as a photoconductive element. The structure works as a switch that controls propagation of 0.6 THz beam by ultra-short optical laser pulses. The device operates as a one-dimensional photonic crystal with GaAs core acting as a resonant defect layer. The THz electric field is enhanced in the photonic structure

at the GaAs layer. Due to small wavelength of THz beam and small size of structure, the laser beam-width could also be small. The response time of the element to pulsed photoexcitation is about 130 ps, which is nearly 80 periods of oscillations in the THz wave beam.

Further progress in the light control of THz beams is reported in [3]. The authors demonstrate manipulation of THz waves by photoconductive gratings induced in a GaAs layer by femtosecond laser pulses. The pattern of photoexcited carriers can create dynamical diffractive elements, thus, providing a route to THz components with reconfigurable functionality.

All the devices above require high-power lasers for their operation. While it is needed for ultra-fast devices, this poses limitations in the research on physical effects in light-controlled systems, optimization of design and functionality of devices, development of more efficient structures, and in those cases when slower but more sensitive switches are required.

The aim of this work is to present the experimental implementation of mm-wave quasi-optical beam switch controlled by the LED array light pulses easily created with inexpensive equipment.

In distinction from other research, we work in a different frequency range which is the mm-wave band of 75-110 GHz (W-band) rather than sub-millimeter waves of about 0.6 THz used in [2]. Further, we perform direct frequency domain measurements using a vector network analyzer (VNA) as an alternative to the time domain approach developed in [2]. We employ different materials and kinds of structures providing much higher quality factors (Q-factors) and, therefore, many orders of magnitude greater sensitivity. Finally, we apply easily available and inexpensive optical sources such as a set of four 100 W LED arrays as compared to special high-power ultra-short-pulse lasers.

Light-controlled quasi-optical switches could find potential applications in telecommunication (opto-electronic modulation of THz beams, enhanced sensitivity of THz array sensors), quasi-optics with dynamical diffractive elements (polarization cryptography), optically reconfigured antennas (ultra-fast beam scanning), circuit protection from optical and electromagnetic pulses, etc. Particular benefits of the given design are, mainly, for the research purpose thanks to essential compatibility with common laboratory equipment and simplicity of implementation that will boost the research in all the related areas.

2. Bragg structures with resonant transmission

Using Bragg structures with resonant transmission is a practical way of making photonics-enhanced light-controlled switches for mm-wave beams. A structure of this kind contains a layer of low-loss semiconductor (e.g., high-resistivity silicon) that creates a narrow transmission peak at a certain frequency within the mm-wave propagation gap [Fig. 1]. The height of the peak is sensitive to the intensity of light illuminating the structure, thus providing the light control of propagation at the peak frequency. The sensitivity increases with increasing the Q-factor of the structure evaluated at that frequency.

For observing the band gap with propagation peaks in the frequency band of 75 to 110 GHz, we used Bragg structures made of fused quartz wafers separated with air spaces of carefully selected thickness (about 0.5 mm) and a silicon wafer as a defect layer. Using a silicon wafer with resistivity of 30 KOhm · cm allowed us to make the structures with $Q \approx 550$ at the resonant transmission peak about 90 GHz in the propagation gap centered between 75 and 110 GHz (for the comparison, an estimate for 0.6 THz structures in [2] shows $Q \approx 36$).

High resistivity of silicon is usually linked with high photoconductivity due to long recombination lifetime in a pure material [4]. The latter is a limiting factor in the recovery of mm-wave propagation after the pulse decay, though it does not hamper the speed of blocking the beam when the light pulse is arriving.

MM-wave measurements were made using a VNA-based quasi-optical bench facility developed at the Maynooth University Department of Experimental Physics (Ireland). The VNA (R&S ZVA24) is equipped with frequency extension head (ZVA-Z110) for W band operation.
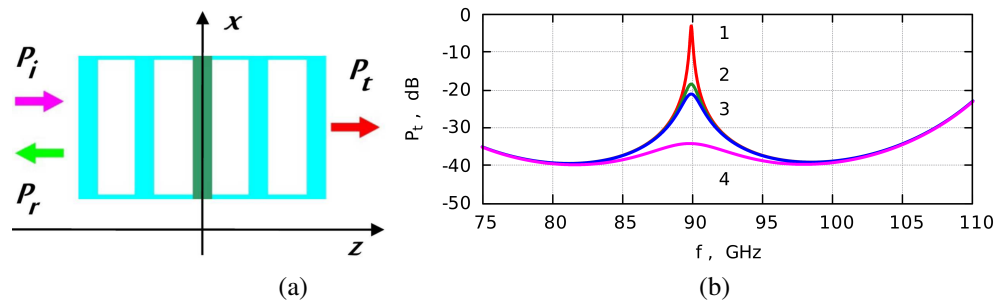
Fig. 1. (a) Schematics of a Bragg structure and (b) simulations of mm-wave transmission where curves 1 to 4 show the frequency spectrum of transmitted power P_t in the dark state (curve 1) and under the illumination of increasing intensity (curves 2, 3, and 4, respectively)

The bench is equipped with custom split-step dual-aspheric mm-wave Fresnel lenses [5] and a top-frame LED-array light source designed for the optimal operation of the setup [Fig. 2].
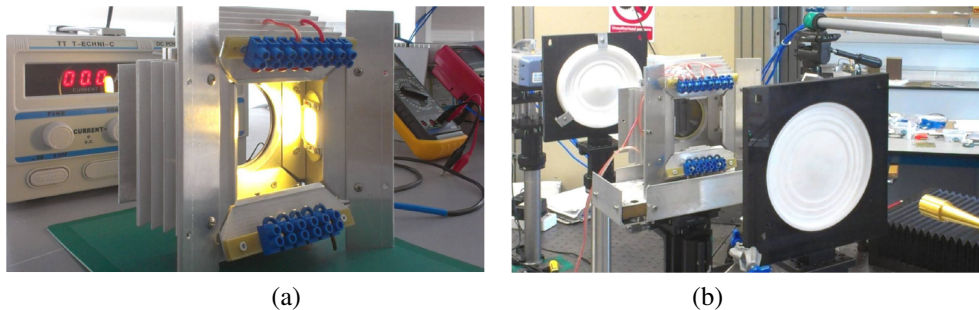

Fig. 2. (a) A top-frame LED-array light source and (b) W-band quasi-optical setup used for the light-controlled mm-wave experiments at the NUI Maynooth, Ireland

Having the structures of high quality allowed us to observe optical switching of mm-wave beams with various light sources including 250 W infrared incandescent and 500 W halogen lamps, a set of a few 100 W LED arrays, and a stroboscopic photo-flash lamp. The LED arrays are found to be the most suited among the other sources considered since they could be used in a pulse mode and, though producing smaller peak power compared to the flash lamp, could generate shorter pulses (down to 100 ns according to specification) and provide a better control of power and timing characteristics (the other sources create a smaller response and cannot be placed close to the switch aperture). Experiments of this kind are complementary to other research which concern light-controlled whispering-gallery-mode resonators [6] composed of the same wafers for the comparison of alternative developments in this area.

3. Simulations of beam transmission through Bragg structures

Simulations of mm-wave propagation through multi-layer structures are based on the plane-wave transmission matrix approach extended for spatially-limited vector electromagnetic beams. Figure 1(b) shows the results obtained for the structure denoted as 4(qa)-s-4(aq) where 4(qa) means a set of four quartz wafers q separated with air spaces a (each of thickness q = 0.496 mm and a = 0.695 mm, respectively) and s is a silicon wafer (s = 0.500 mm). Curves 1 to 4 show the frequency spectrum of transmitted power P_t in the dark (1) and under the illumination (2-4) in the case of normal incidence of plane mm-waves on the photonic structure. The material

parameters fitting the experiments are $\varepsilon_q = 3.83 \pm 0.01$ and $\tan(\delta_q) \le 0.001$ for the fused quartz and $\varepsilon_s = 11.85 \pm 0.09$ and $\tan(\delta_s) \le 5 \cdot 10^{-5}$ for silicon in the dark state.

Photoconductive layer in a silicon wafer is represented in our model as a layer of uniform conductivity σ with effective thickness l. In this model, curves 2 and 3 correspond to the electron (hole) concentration in quasi-neutral photoconductive layer $n_2 = 5 \cdot 10^{13} \text{cm}^{-3}$ and $n_3 = 1 \cdot 10^{14} \text{cm}^{-3}$ at the layer thickness $l_2 = 0.2$mm and $l_3 = 0.1$mm, respectively, and curve 4 corresponds to $n_4 = 5 \cdot 10^{14} \text{cm}^{-3}$ at $l_4 = 0.1$mm. The difference between curves 2 and 3 shows the effect of a different thickness l at the constant total number of photoexcited carriers when their surface density is $n_{s_2} = n_{s_3} = 10^{12} \text{cm}^{-2}$. For the comparison, the recombination lifetime in our wafers is estimated to be about $\tau = 30\mu$s which yields the ambipolar diffusion length $L = 0.27$mm, whereas the light absorption length is $l_a = 2\mu$m at the wavelengths of the LED array source [4] (at the light pulses used in our experiments, the effects occur in the regime of developed electron-hole diffusion when the effective layer thickness l is close to the diffusion length L).

For computing spatially-limited beams propagating through multi-layer structures, we used a vector plane wave spectrum representation of beams proposed in [7, 8]. Assuming the incident beam is linearly polarized along the x-axis, see Fig. 1(a), and has an axially symmetric plane-wavefront Gaussian profile of the E_x electric field component at the aperture, we recovered all the $\vec{E}$ and $\vec{H}$ field components of partial plane waves satisfying Maxwell's equations. Then, propagating the partial plane waves through the structure and using Fourier transform for recovering transmitted and reflected beams, we simulated propagation and reflection of beams of the given profile by multi-layer structures. The extension of simulations for spatially-limited beams and oblique plane wave incidence was employed for the estimates of various imperfections of real systems.

4. High-power LED array as a light source

A custom light source was developed for making the measurements with light pulses of adjustable duration (potentially down to $\sim 1\mu$s) and enhanced power when required. The source was built around an LED array made of four chip-on-board LED modules, with nominal power of 100 W per chip. The modules were mounted in a top-frame assembly in close proximity to the structure to be illuminated, without obstructing it, see Fig. 2. The modules were arranged symmetrically along the perimeter of aluminum assembly, each module being fixed at the mid-point of the relevant heat-sink section. The light is directed towards the Bragg structure in the middle of the aperture of the diameter $D = 68$mm providing the illumination of a silicon layer through a set of four quartz wafers on the front part of the structure.

The benefit of making Bragg structures of quartz wafers is that the latter have an excellent transparency in both the mm-wave and the optical bands, including the near infrared and ultraviolet parts of spectrum. The light reflection from the whole structure with a silicon layer inside is still significant and makes about 50% throughout the optical band of interest as measured at the normal incidence of the light beam (we did not use any antireflection coatings at this stage of research).

We tested the light intensity across the aperture between the mid-points of the opposite sides of LED assembly. The light intensity was found to be uniform within 2% across the aperture, being about 0.5W/cm^2 at the LED specification voltage $U = 36$V as measured with a pin-diode photodetector SFH203P. Figure 3 shows (a) the spectral energy density of the LED light in comparison to blackbody radiation at the temperature $T = 5000$ K (curves 1 and 2, respectively) and (b) current-voltage (curve 1) and light-voltage (curve 2) characteristics of the LED array light source.

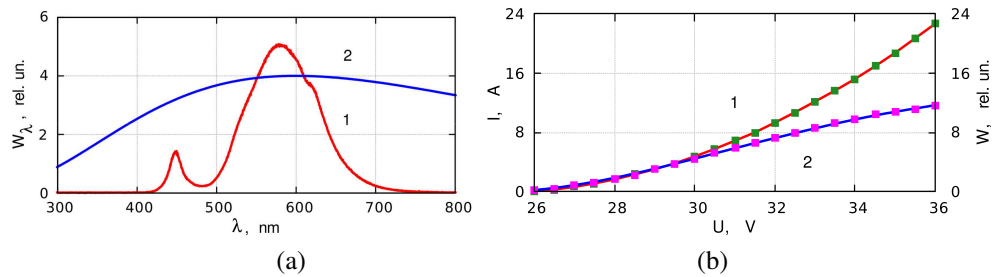Fig. 3. (a) Spectrum of the LED compared to blackbody radiation ($T = 5000$ K) and (b) pulse mode current-voltage I-U and light-voltage W-U characteristics of the LED array

5. Dielectric material characterization with Bragg structures

As the first step, we measured mm-wave transmission and reflection spectra of Bragg structures with different numbers of quartz wafers and varying thickness a of air spaces. We also tested Bragg structures with one, two, and three quartz wafers used as a defect layer instead of silicon [curves 1 to 3 in Fig. 4(a), respectively, in case of $a = 0.508$ mm and wider spaces $u = 1.205$ mm around the defect layer]. Through comparison with simulations, we found dielectric parameters of the fused quartz being used (the electric fused quartz for RF applications). In a similar way, we recovered the dielectric parameters of silicon (see values provided in Section 3).

Basic parameters that control the effects are the configuration of the structure, the thickness of layers, and the values of real and imaginary parts of complex dielectric constants of the layer materials. For the structure of given geometry, the real and imaginary parts of dielectric constants define the frequency position and the spectral width of transmission peak, respectively.
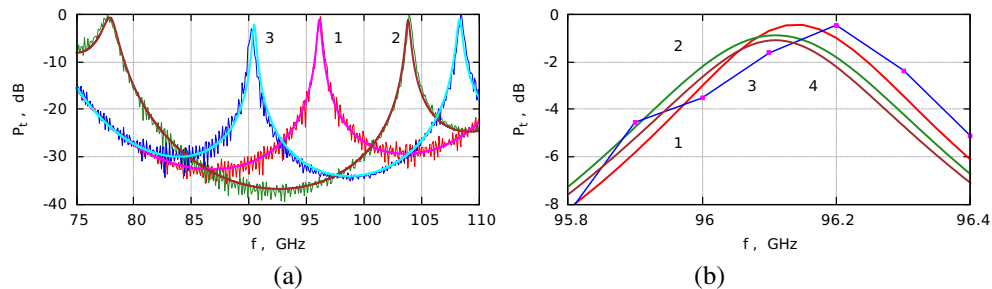

Fig. 4. (a) Transmission spectra of structures with one, two, and three quartz wafers as a defect layer (smooth and dithered curves correspond to simulations and experiments, respectively) and (b) the effects of beam width $w_A = 24$mm and wafer non-flatness $\sigma = 1\mu$m (no absorption) compared to the experiment and plane wave incidence (with absorption) at the same other parameters of quartz structures (curves 1 to 4, respectively)

We evaluated the effects of various imperfections emerging in the experiments as compared to simplified models. They include the imperfect knowledge of thickness of quartz wafers and air spaces, smooth variations of thickness across the wafers (non-flatness), limited mm-wave beam width, slightly oblique beam incidence, inaccurate evaluation of material dielectric constant and loss tangent. The imperfections could affect both the frequency position and the spectral width (Q-factor) of transmission peak of a defect-layer structure [Fig. 4(b)].

We verified that all the quartz wafers have the same thickness with the accuracy no worse then 1μm at any point from the center to the very rim. So, as a benchmark, we considered two kinds of effect that could easily be simulated and detected experimentally. The first kind was the

frequency shift of the transmission peak due to imperfections, as compared to the effect of $1\mu m$ error in the thickness of perfectly flat, uniform, identical, and lossless wafers. The other kind was the widening of the transmission peak in structures with imperfections, when compared to the ideal structures having the loss tangent of quartz wafers $\tan(\delta_q) = 0.001$.

The effects of various imperfections were evaluated separately. We found the frequency shift of transmission peak $\delta f = \mp 0.05\text{GHz}$ arises due to variation of parameters $\delta a = \pm 1\mu m$, $\delta q = \pm 0.6\mu m$, $\delta\varepsilon_q = \pm 0.01$ (in quartz structures), $\delta s = \pm 0.4\mu m$, and $\delta\varepsilon_s = \pm 0.02$ (the actual uncertainty of s is $\delta s = \pm 2\mu m$ providing $\delta f = \mp 0.22\text{GHz}$ and $\delta\varepsilon_s = \mp 0.09$). A similar positive shift $\delta f = +0.05\text{GHz}$ appears due to uncertainty of the angle of incidence of plane waves $\delta\theta = \pm 2\text{deg}$ and for the actual Gaussian beam incidence as compared to the plane waves [Fig. 4(b)] when the beam neck radius at the structure aperture is $w_A = 24\text{mm}$ [5] (the aperture radius is $R = 34\text{mm}$). For comparison, the full width of transmission peak at the frequency $f = 96.1$ GHz [curve 1 in Fig. 4(a)] is $\Delta f = 0.34$ GHz ($Q = 280$).

Smooth random variations of thickness across the layers (non-flatness) would produce, at the given mean values of thickness, and in absence of absorption losses, a broadening of transmission peaks (the reduction of Q-factors) instead of systematic frequency shift. For Gaussian non-flatness of layers with standard deviation $\sigma = 1\mu m$ in a quartz structure with no absorption, the estimate of the effect is the same as for the structure of perfectly flat layers at the loss tangent of quartz $\tan(\delta_q) = 0.001$. This is the case observed in the experiments. So, the effect could be attributed to either the absorption losses or non-flatness of layers. Therefore, the absorption parameters specified above should be considered as the upper limits being detected.

6. Light-controlled silicon-based photonics-enhanced mm-wave switches

Having created Bragg structures of enhanced sensitivity, we made VNA measurements of mm-wave transmission and reflection spectra of silicon-based devices in their response to the light pulses of various intensity generated by the LED array source.

The VNA measurements impose limitations on the duration of light pulses. At the highest bandwidth setting, the VNA needs $\tau_{VNA} = 110\mu s$ for taking a record of a single parameter value (e.g., S_{21}) at a single frequency point. The light pulse duration τ_p should exceed the time τ_{VNA}. So, we are confined to a regime of developed electron-hole diffusion when τ_p is greater than the recombination lifetime $\tau = 30\mu s$ and the photoconductive layer is expanded over the diffusion length $L = 0.27\text{mm}$ (for the layer to expand from $l_a = 2\mu m$ to, e.g., $l = 10\mu m$, it takes $\delta t \sim 40ns$). Being restricted to the diffusion mode, we used Sorensen DCS33-33 power supply for driving the LED array source with pulses of $\tau_p = 8\text{ms}$ and selected a reduced VNA bandwidth for improving the accuracy of the VNA data.

The results of the VNA measurements are presented in Fig. 5. They confirm high sensitivity of transmission peak observed at the frequency of 90GHz to the light power of our source. This shows a possibility of optical control of mm-wave beams propagating through the devices at the chosen resonant frequency with the light emitted by the LED sources. It is worth noting that the high power of light sources is only needed for creating a high peak power at the limited total energy of pulses. At pulse duration $\tau_p = 100\mu s$ and the light power flux 0.5W/cm^2 of the LED array mentioned above, we would have the pump fluence $\Phi = 50\mu\text{J/cm}^2$ which is in the same range as those values obtained with femtosecond lasers in [1–3].

A benefit of the VNA measurements is the direct recording of both the magnitude and the phase of transmitted and reflected signals. Figure 6 shows the phase of measured and simulated S_{21} transmission signal as a function of frequency in the dark state and under the LED array illumination. Using either the phase or the power data, we could find both the Q-factor and the mm-wave photon lifetime τ_{PC} in the given photonic structure. With the power data, e.g., we find $Q = f/\Delta f = 550$ and $\tau_{PC} = 1/(\pi\Delta f) = 6.25\text{ns}$ where $\Delta f = 0.16$ GHz is the full width at half magnitude of the resonant transmission peak. These values show the potential of nanosecond
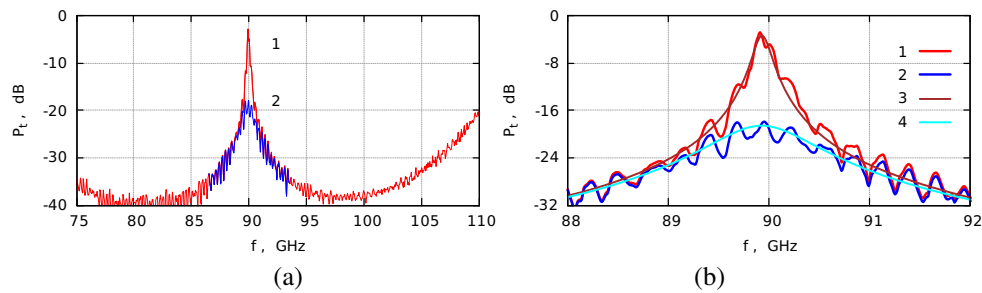
Fig. 5. Light-sensitive transmission peak of a Si-loaded structure at the frequency f = 90 GHz when (a) measured in the dark and in the light of the LED-array at the voltage U = 36 V (curves 1 and 2, respectively, with account of reference signal of free-space propagation) and (b) simulated at the Gaussian beam incidence [curves 3 and 4, which are similar to plane-wave cases 1 and 2 in Fig. 1(b), respectively]
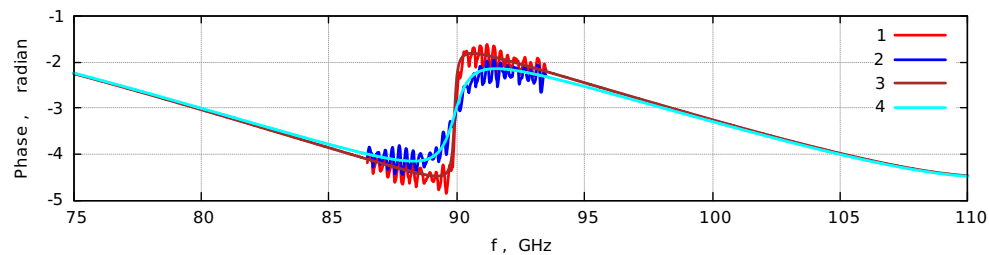
operation of the devices being considered.

Fig. 6. Phase as a function of frequency of measured (curves 1 and 2) and simulated (curves 3 and 4) transmission signal through the structure in the dark state (curves 1 and 3) and under the LED array illumination (curves 2 and 4, U = 36 V) evaluated with respect to the reference signal of free-space propagation

The amplitude of peak modulation exceeding the level of 15 dB is observed with the given structures at the LED array illumination. It means the structures could be used with many other light sources (e.g., the light of conventional 100 W incandenscent lamp created the modulation at the level of 3 dB). At the dynamic range of 15 dB, the device can be used as a light-controlled attenuator of mm-wave beams (with a brighter light, the dynamic range is increasing). One may compare it with a 50% modulation (3 dB drop in transmission) of an 0.6 THz switch in [2], though the latter is operating on a much faster (100 ps) time scale.

When simulating the device performance, we observed that an estimate of photoelectron density based on the measured light intensity shows the values more than an order of magnitude greater than those used for computing the plots in Fig. 1. That means the observed effect is smaller than expected. This could arise from excessive reflection of light due to oblique incidence, non-uniform distribution of photocarriers, significant surface recombination, etc. On the other hand, this also shows a possibility of further enhancement of sensitivity. The frequency position of transmission peak obtained with available wafers could also be varied. This is achieved through increasing or decreasing the air spaces between the inner silicon layer and the outer blocks of Bragg structure. In practice, a set of four quartz wafers on each side of a silicon wafer is found to be optimal for the best operation of the entire setup.

7.   Conclusions

We developed light-controlled photonics-enhanced quasi-optical mm-wave beam switches oper-
ating at resonant frequencies in the mm-wave band of 75 to 110 GHz. The switches were built as
the Bragg structures composed of a stack of fused quartz wafers with a resonant defect layer of
high-resistivity silicon that creates a narrow transmission peak at a certain frequency within the
mm-wave propagation gap. The structures are controlled by a dedicated 400 W LED array light
source. A resonant mm-wave transmission peak modulation exceeding the level of 15 dB has
been achieved with these structures in response to the LED array light-pulse excitation.

Acknowledgments